Damage-Mitigating Control of a Reusable Rocket Engine: Part I—Life Prediction of the Main Thrust Chamber Wall

Xiaowen Dai

Asok Ray
Fellow ASME

Mechanical Engineering Department,
The Pennsylvania State University,
University Park, PA 16802

The goal of damage-mitigating control in reusable rocket engines is to achieve high performance without overstraining the mechanical structures; and the major benefit is an increase in structural durability with no significant loss of performance. This sequence of papers in two parts investigates the feasibility of damage mitigating control of a reusable rocket engine similar to the Space Shuttle Main Engine (SSME). The challenge here is to characterize the thermo-mechanical behavior of the structural materials for damage prediction in conjunction with dynamic performance analysis of the thermo-fluid process in the rocket engine, and then utilize this information in a mathematically and computationally tractable form for synthesizing decision and control algorithms. This paper is the first part and investigates the damage phenomena in the coolant channel ligament of the main thrust chamber of a rocket engine that are characterized by progressive bulging-out and incremental thinning leading to eventual failure by tensile rupture. A creep damage model is analytically derived based on the theories of sandwich beam and viscoplasticity. The objective of this model is to generate a closed-form solution of the wall thin-out in real time where the ligament geometry is continuously updated to account for the resulting deformation. The creep damage model has been examined for both single-cycle and multi-cycle stress-strain behavior, and the results are in agreement with those obtained from the finite element analyses and experimental observation. Due to its computational efficiency, this damage/life prediction model is suitable for on-line applications of decision and control, and also permits parametric studies for off-line synthesis of damage mitigating control systems. The second part, which is a companion paper, develops an optimal policy for damage mitigating control of the rocket engine.

Introduction

In order to achieve high performance with enhanced reliability, availability, component durability, and maintainability, rocket engine control systems need to be synthesized by taking performance, mission objectives, service life, and maintenance, and operational costs into consideration. However, the current state-of-the-art of control systems synthesis for rocket engines focuses on improving dynamic performance and diagnostic capabilities based upon the assumption of conventional materials with invariant characteristics. Lack of appropriate knowledge about the properties of these materials will lead to either less than achievable performance due to overly conservative design, or over-straining of the structure leading to unexpected failures and drastic reduction of the useful life span. For example, the original design goal of the Space Shuttle Main Engine (SSME) was specified for 55 flights before any major maintenance, but the current practice is to disassemble the engine after at most a few flights for maintenance. To this effect, the motivation and concept of damage-mitigating control in rocket engines have been introduced in recent publications, namely, Lorenzo and Merrill (1991a) and Ray et al. (1994a, 1994b), with the objective of achieving high engine performance without overstraining the mechanical structures.

Figure 1 shows a conceptual view of the damage-prediction system, which is an essential ingredient of the proposed damage-mitigating control system. The plant model is a finite-dimensional state-space representation of the process dynamics (e.g., thermo-fluid dynamics of the rocket engine). The plant states are inputs to the structural model which, in turn, generates the necessary information for the damage model. The output of the structural model is the load vector which may consist of time-dependent variables such as stress, strain, and temperature at the critical point(s) of the structure. The damage model is a continuous-time representation of life prediction such that it can be incorporated within the framework of the control system in the state-variable setting. The objective is to include the effects of damage rate and damage accumulation under time-dependent thermo-mechanical loading. The damage state vector $\mathbf{v}(t)$ indicates, for example, the level of creep and fatigue damage accumulation at one or more critical points, and its time derivative $\dot{\mathbf{v}}(t)$ indicates how the instantaneous load is affecting the structural components (Ray and Wu, 1994a, 1994b). The plant dynamic model in Fig. 1 is unaffected by accumulated damage and hence there is no inherent damage feedback as seen in Fig. 1. The rationale is that the physical phenomenon of material damage in a plant component does not alter its macroscopic mechanical behavior (such as stiffness constant) within the service life span. An example is fatigue-induced microcracks in a turbine blade that do not alter the natural frequency until the end of its useful life. That is, when a change in the frequency becomes detectable, the blade life is almost expended. The damage information is useful for intelligent decision-making such as failure prognosis and risk analysis (Lorenzo and Merrill, 1991b; Ray et al., 1994b; and Ray and Wu, 1994a, 1994b).

Contributed by the Dynamic Systems and Control Division for publication in the JOURNAL OF DYNAMIC SYSTEMS, MEASUREMENT, AND CONTROL. Manuscript received by the DSCD March 15, 1994; revised manuscript received June 28, 1995. Associate Technical Editor: J. L. Stein.

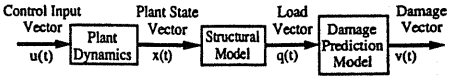

Fig. 1 Damage prediction system

This two-part paper investigates the feasibility of damage mitigating control of a reusable rocket engine such as the Space Shuttle Main Engine (SSME). The critical components of the SSME, which potentially limit its functional life, include the following (Sutton, 1992):

- Blades of the fuel turbine;
- Blades of the oxidizer turbine;
- Main thrust chamber wall cooled by liquid hydrogen;
- Rocket nozzle wall cooled by liquid hydrogen; and
- Injector tubes carrying the turbine exhaust gas into the combustion chamber.

The fatigue failure in the injector tubes, originally caused by thermal stresses, has been reportedly solved by appropriate selection of materials in the later versions of the SSME. Therefore, the injector tube is not included as a critical component in the present study. The failure of the coolant channel ligaments in the main thrust chamber and rocket nozzle are caused by creep and creep ratcheting due to plasticity of copper (and copper alloys) at a high temperature (for example, ~1200°R). Since the ligament temperature at the main thrust chamber is higher than that at the nozzle, the damage control of the combustor chamber wall is expected to protect the nozzle wall. Therefore, the first three components, namely, blades of the fuel turbine, blades of the oxidizer turbine, and coolant channel ligaments at the main combustion chamber, are considered as the critical points for damage mitigating control of a reusable rocket engine in the work reported here.

This paper, which is the first of a sequence of two parts, presents the development of a structural model and a damage model of the coolant channel ligament based on the theories of sandwich beam (Robinson and Arnold, 1990) and thermo-viscoplasticity (Freed, 1988). The second part (Dai and Ray, 1996), which is a companion paper, develops an open-loop control policy via optimization of a cost functional of the plant dynamic performance without violating the damage constraints in the above three critical components. This is an extension of our previous work (Ray et al., 1994c) which reports damage-mitigating control of a reusable rocket engine with the fuel and oxidizer turbine blades as the critical components.

Structural and Damage Models

Life prediction models of the coolant channel ligament in the main thrust chamber of the SSME have been reported by several investigators (Hannum et al., 1976; and Quentmeyer, 1977). It was revealed that the progressive deformation indicated by incremental bulging-out and thinning of the ligaments occurs before the development of a fatigue failure. This is especially true for copper (and copper alloys) during the heating and cooling processes associated with each cycle of engine operation. Therefore, the prime cause of coolant wall failures is identified as creep rupture enhanced by ratcheting. Various approaches have been reported in literature for life prediction modeling of the coolant channel ligament. Finite element methods are available for analyzing inelastic structures of complex geometry such as the coolant channel ligament under cyclic loading (Armstrong, 1981; Kasper, 1984; and Arya, 1992). However, for on-line damage-mitigating control, the finite element approach is not practicable because of exceptionally large requirements of computational resources. An attempt was made by Porowski et al. (1985) to formulate a life prediction model of the chamber wall based on the elasto-plasticity theory by simplifying the coolant channel ligament as a rectangular beam. However, this method is not suitable for the damage-mitigating control system because the intra-cycle incremental bulging-out and thinning cannot be evaluated in this model.

A simplified analytical model has been formulated in this paper for damage prediction of the main thrust chamber. The proposed model employs the sandwich beam approximation which was used by Robinson and Arnold (1990) to investigate

Nomenclature

A = cross-sectional area, constant in the viscoplastic model
a_{11}, b_{11}, d_{11} = coefficients in stiffness matrix
B = back stress
d = core thickness of the sandwich beam
d_1, d_2 = distance between the top or bottom of the thin faces to the beam mid-plane in the sandwich beam
D = damage measure, drag stress
D_o = material constant
E = modulus of elasticity
h = inelastic material constant
H = inelastic material constant
k = Boltzman constant
l = half length of the beam
L = limiting value of the back stress
M = bending moment
N = tensional force, total number of steps
n = material parameters
P = pressure
p = distributed force per unit length
Q = activation energy
r = recovery function in the viscoplastic model
S = deviatoric stress, material constant
T = absolute temperature
t = time
w = radial deflection at the mid-plane of the beam
u = axial displacement
$\mathbf{v}$ = damage state vector
x, y, z = Cartesian coordinates
Z = Zener-Hollomon parameter in the viscoplastic model
α = coefficient of thermal expansion
δ_1, δ_2 = radial deflection of the two faces of the ligament
ϵ = normal strain
ϑ = actual thickness of the coolant channel ligament
Φ = function
ϕ = curvature angle in the sandwich beam
η, ξ = dummy variable in the integration
κ = midplane curvature
θ = thickness of each face in the sandwich beam
Θ = thermal diffusivity function,
τ = thinning of the ligament, shear stress
$\Im$ = remaining service life
σ = stress
Σ = effective stress

Superscripts

e = elastic part
o = midplane
p = plastic part
th = thermal part

Subscripts

1 = coolant side surface of the coolant channel ligament
2 = hot-gas side surface of the coolant channel ligament
B = close-out wall
f = useful service period
m = melting point
o = initial value, reference point, reaction load

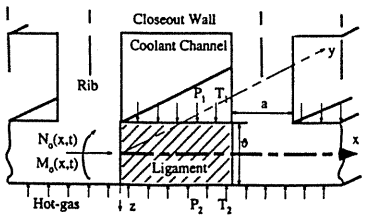

Fig. 2 Rectangular beam model of the coolant channel ligament

the influence of dynamic and thermal recovery mechanisms on creep buckling. In the present paper, the progressive changes in the ligament geometry and the nonlinear effects of creep and plasticity interactions are taken into account for calculation of inelastic stress-strain relations and life prediction. The proposed model, hereafter called the sandwich beam model, captures the inelastic strain ratcheting, progressive bulging-out and incremental thinning phenomena in the coolant channel ligament via the thermo-viscoplastic model of Freed (1988). A salient feature of the sandwich beam model is numerical efficiency which is essential for damage-mitigating control.

Formulation of an Equivalent Sandwich Beam Model. The structural model of the coolant channel ligament is based on the experimental prototype of the cylindrical thrust chamber by Quentmeyer (1977), which was designed to emulate the operating conditions of the SSME. The cross-sectional dimensions of the thrust chamber configuration are geometrically similar to those of a full scale thrust chamber of the SSME even though the diameter and length of the nozzle are reduced. An enlarged view of the 72 coolant channels described by Quentmeyer (1977) are shown in Fig. 2, where the ligament connects two consecutive ribs forming the inner wall of the thrust chamber. The ligament is constructed from oxygen-free high conductivity (OFHC) copper, and the close-out wall is made of electroformed copper. A more advanced material called, NARloy-Z, which is a copper-zirconium-silver alloy, is currently used as the ligament material in the SSME (Dai and Ray, 1995; Ray and Dai, 1995).

To focus on the interactions between the structural response and temperature dependence of the coolant channel ligament, governing equations are derived using Bernoulli's assumption based on the small deflection theory and by neglecting deformations due to shear. The coolant channel ligament of rectangular cross-section in Fig. 2 is represented by an idealized sandwich beam model. The coordinates of the sandwich beam model (Robinson and Arnold, 1990) and its loading conditions are shown in Fig. 3 where x, y, and z coordinates correspond to the circumferential (hoop), axial, and radial directions of the ligament, and the subscripts 1 and 2 denote the cold and hot side of the ligament, respectively. The sandwich beam model consists of two thin faces with equal thickness, θ, which are separated by a rigid and incompressible core of thickness $d_1 + d_2 - 2\theta$. Consequently, the local bending stiffness of the thin faces are neglected, the normal stresses σ_1 and σ_2 are assumed to be constant throughout the faces, and the core resists shear deformations and bears no normal stresses. The ligament is exposed to the hot hydrogen-rich gases of combustion on one surface and the cryogenic hydrogen coolant on the other surface. The surfaces are also subjected to hydrostatic pressure which exerts distributed force on the wall in the radial (z) direction. The time-dependent temperature and pressure on the coolant side of the ligament are denoted as $T_1(t)$ and $P_1(t)$, and on the hot-gas side as $T_2(t)$ and $P_2(t)$, respectively. Considering a unit length of the ligament in the axial (y) direction, the uniformly distributed load on the beam is denoted as $p(t) = P_1(t) - P_2(t)$ in the radial (z) direction. Although the ligament temperature is essentially invariant along the x-direction because of geometrical symmetry, there exists a thermal gradient across the wall thickness in the radial (z) direction. Due to the symmetric loading and geometric configuration, only a half-beam model of length l needs to be considered where $2l$ is the length of the ligament in the circumferential (x) direction.

For the sandwich beam model to be equivalent to the ligament structure of rectangular cross-section in terms of identical deformation in the hoop and radial directions at the mid-plane, the parameters d_1, d_2, A_1, and A_2 of the sandwich beam, shown in Fig. 3, are chosen such that the cross-sectional area and moment of inertia of the rectangular beam are preserved (Arnold and Robinson, 1989) as:

$$d_1 + d_2 = d = \frac{\vartheta}{\sqrt{3}}; \quad \text{and}$$

$$A_1 = A_2 = A = \frac{\vartheta}{2} \quad \text{for unit length in the } y\text{-direction} \quad (1)$$

where ϑ is the true thickness of the rectangular beam (i.e., the actual coolant channel ligament thickness), d_1 and d_2 are the distances from the centroids of the two faces to the mid-plane, A_1 and A_2 represent the cross-sectional areas of coolant side and hot-gas side of the ligament for unit length in the y-direction, respectively.

Kinematic Assumptions. Based on the symmetric geometry of the sandwich beam model in Fig. 3, the expressions for the total strain-displacement relation are as follows:

$$\epsilon^{\text{tot}}(x, t) = \epsilon^o(x, t) + (-1)^i d_i \kappa(x, t); \; i = 1, 2;$$

$$\text{and} \quad w(x, t) = w^o(x, t) \quad (2)$$

where $u^o(x, t)$ and $w^o(x, t)$ denote the displacement and deflection at the mid-plane $z = 0$, respectively. The mid-plane strain ϵ^o and mid-plane curvature κ are defined as:

$$\epsilon^o(x, t) = \frac{\partial u^o(x, t)}{\partial x}; \quad \text{and} \quad \kappa(x, t) = -\frac{\partial^2 w(x, t)}{\partial x^2} \quad (3)$$

Constitutive Equations. A sizable body of literature exists on phenomenological constitutive equations for the strain rate and temperature dependent plastic deformation behavior of metallic materials. Almost all of these unified theories are based on small strain assumptions. More than ten unified constitutive theories have been reviewed by Chen et al. (1984). Allen and Beek (1984) reviewed and clarified the general theory of internal state variables for application to inelastic metals in high temperature environments. McDowell (1992) extended the concept of nonlinear kinematics hardening model for multiple back stress under thermo-mechanical cyclic loading.

The viscoplastic theory has been adopted for modeling the nonlinear inelastic material properties at high temperatures because of its ability to represent both rate-dependent creep and rate-independent plastic behavior. The general theory of a multiaxial viscoplastic model is reported by Freed (1988), and the model parameters have been identified for OFHC copper by Freed and Verrilli (1988). This viscoplastic model serves as

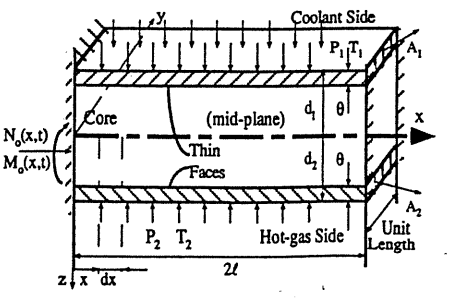

Fig. 3 Sandwich beam model of the coolant channel ligament

the constitutive law with a single kinetic equation and two types of internal state variables, namely, the tensorial anisotropic back stress B_{ij} (which is deviatoric) and the scalar isotropic drag stress D. In addition to the assumptions of small displacements and deformations, and absence of coupling between the static and dynamic recovery terms in the viscoplastic model, the major assumptions for modeling the sandwich beam in the present analysis are as follows:

(i) the curvature of the ligament of a single coolant channel is neglected in the undeformed condition due to a large number of such channels;

(ii) the modified version of the viscoplastic constitutive equations of the Freed's model is presented only for the two thin faces of the sandwich beam structure where $\tau_{xz} = 0$ and $\sigma_z = 0$;

(iii) for stress components in the axial (y) direction are negligible (i.e. $\sigma_y, \tau_{xy}, \tau_{zy} = 0$);

(iv) the total strain ϵ^{tot} is assumed to be the sum of elastic, inelastic, and thermal strains, ϵ^e, ϵ^p, and ϵ^{th} on each of the cold side and hot side faces, i.e.,

$$\epsilon_i^{tot}(x, t) = \epsilon_i^e(x, t) + \epsilon_i^p(x, t) + \epsilon_i^{th}(x, t) \qquad i = 1, 2 \quad (4)$$

(v) for the one-dimensional loading problem in the sandwich beam, the hoop stresses in the cold and hot faces are obtained by combining Eqs. (2) and (4) as:

$$\sigma_i = E_i(\epsilon^o - d_i\kappa) - E_i\epsilon_i^p - E_i\epsilon_i^{th}; \quad i = 1, 2 \quad (5)$$

The deviatoric stress tensor S_{ij} and the effective stress tensor Σ_{ij} at the two faces of the sandwich beam are defined as follows:

$$S_{ij} = \sigma_{ij} - 1/3\sigma_{kk}\delta_{ij}; \quad \text{and} \quad \Sigma_{ij} = S_{ij} - B_{ij} \quad (6)$$

The inelastic hoop strain rate relations at the two faces of the sandwich beam are given by the flow law as:

$$\dot{\epsilon}_{ij}^p = \Theta Z \frac{\Sigma_{ij}}{\|\Sigma\|_2} \quad (7)$$

where $\|\Sigma\|_2 = \sqrt{(\Sigma_{ij}\Sigma_{ji})/2}$ is the l_2-norm of the effective stress tensor. The thermal-diffusivity function Θ and the Zener-Hollomon parameter Z are defined as:

$$\Theta = \begin{cases} \exp(-Q/kT) & T \geq 0.5T_m \\ \exp\left\{\dfrac{-2Q}{kT_m}\left[\ln\left(\dfrac{T_m}{2T}\right) + 1\right]\right\} & T \leq 0.5\,T_m \end{cases};$$

$$\text{and} \quad Z = \begin{cases} AF^n & F \leq 1 \\ A\exp[n(F-1)] & F \geq 1 \end{cases} \quad (8)$$

where Q is the activation energy, k is the Boltzman constant; T is the absolute temperature; T_m is the melting point of the material; A and n are material constants; and the dimensionless function F is defined as $F = \|\Sigma\|_2/D$.

The evolutionary laws provide equations for the internal state variables, namely, the back stress B_{ij} and the drag stress D as:

$$\dot{B}_{ij} = H\Theta Z\left(\frac{\Sigma_{ij}}{\|\Sigma\|_2} - \frac{B_{ij}}{L}\right);$$

$$\text{and} \quad \dot{D} = h\Theta\left(\frac{Z}{G} - r(G)\right) \quad (9)$$

where H, L, and h are inelastic material constants, and the recovery function r is defined as:

$$r(G) = \begin{cases} 0 & D = D_0 \\ AG^{n-1} & D > D_0 \quad \text{and} \quad G \leq 1 \\ \dfrac{A}{G}e^{n(G-1)} & D > D_0 \quad \text{and} \quad G \geq 1 \end{cases} \quad (10)$$

where $G = L/S - D$; and S and D_0 are material constants. The following inequality condition of dissipativity must be satisfied at all instants of time for the viscoplastic theory to be thermodynamically admissible (Freed, 1988):

$$r \geq Z\left[\frac{1}{G} - 2\left(F + \frac{\|B\|_2^2}{LD}\right)\right] \quad (11)$$

Equilibrium Equations. Based on the free body diagram of the sandwich beam, the resultant hoop force N and bending moment M are obtained by integrating the stress over the sandwich beam cross section as:

$$N(x, t) = \int_{-d_2}^{d_1} \sigma_x(x, z, t)dz = \sigma_1(x, t)A_1 + \sigma_2(x, t)A_2$$

$$M(x, t) = \int_{-d_2}^{d_1} \sigma_x(x, z, t)zdz$$

$$= \sigma_2(x, t)A_2d_2 - \sigma_1(x, t)A_1d_1 \quad (12)$$

From the equilibrium conditions, $N(x, t)$ and $M(x, t)$ are expressed in terms of the externally applied distributed load $p(t)$, the hoop force N_o and reaction bending moment M_o at the junction of the ligament with the rib (i.e., at $x = 0$ in Fig. 3) as:

$$N(x, t) = -N_o(t)$$

$$M(x, t) = M_o(t) + p(t)lx - \frac{p(t)x^2}{2} \quad (13)$$

where the unknowns N_o and M_o are to be determined from the boundary conditions in this statically indeterminant structure.

Governing Equations. Combining Eqs. (8) and (12), the following constitutive relations are obtained for the sandwich beam in the matrix form:

$$\begin{pmatrix} N \\ M \end{pmatrix} = \begin{bmatrix} a_{11} & b_{11} \\ b_{11} & d_{11} \end{bmatrix}\begin{pmatrix} \epsilon^o \\ \kappa \end{pmatrix} - \begin{pmatrix} N^{th} \\ M^{th} \end{pmatrix} - \begin{pmatrix} N^p \\ M^p \end{pmatrix} \quad (14)$$

where the extensional, flexural-extensional coupling, and bending stiffness coefficients, a_{11}, b_{11}, and d_{11} are defined as:

$$\begin{bmatrix} a_{11} \\ b_{11} \\ d_{11} \end{bmatrix} = \int_{-d_2}^{d_1} E(z)\begin{bmatrix} 1 \\ z \\ z^2 \end{bmatrix} dz = \begin{bmatrix} A_1E_1 + A_2E_2 \\ A_2d_2E_2 - A_1d_1E_1 \\ A_1d_1^2E_1 + A_2d_2^2E_2 \end{bmatrix} \quad (15)$$

and the thermal and plastic "pseudo-force" and "pseudo-moment" quantities are defined as:

$$\begin{bmatrix} N^{th} \\ M^{th} \end{bmatrix} = \begin{bmatrix} A_1E_1\epsilon_1^{th} + A_2E_2\epsilon_2^{th} \\ A_2d_2E_2\epsilon_2^{th} - A_1d_1E_1\epsilon_1^{th} \end{bmatrix};$$

$$\text{and} \quad \begin{bmatrix} N^p \\ M^p \end{bmatrix} = \begin{bmatrix} A_1E_1\epsilon_1^p + A_2E_2\epsilon_2^p \\ A_2d_2E_2\epsilon_2^p - A_1d_1E_1\epsilon_1^p \end{bmatrix} \quad (16)$$

The flexural-extensional coupling coefficient b_{11} does not necessarily vanish since the elastic modulus is a function of the temperature which varies in the z-direction. This indicates that such couplings, similar to that of a laminated composite material, do occur in the event of thermo-viscoplasticity.

Substitution of ϵ^o and κ from Eqs. (3) into Eqs. (14), (15), and (16) and a rearrangement yield the following pair of coupled nonlinear partial differential equations with t and x as independent variables:

$$\frac{\partial u^o(x,t)}{\partial x} = \frac{1}{A_1A_2E_1E_2(d_1+d_2)^2}[(A_1d_1^2E_1 + A_2d_2^2E_2)N(x,t) + (A_1d_1E_1 - A_2d_2E_2)M(x,t)] + \frac{d_2}{(d_1+d_2)}[\epsilon_1^{th}(x,t) + \epsilon_1^p(x,t)] + \frac{d_1}{(d_1+d_2)}[\epsilon_2^{th}(x,t) + \epsilon_2^p(x,t)]$$

$$\frac{\partial^2 w(x,t)}{\partial x^2} = \frac{-1}{A_1A_2E_1E_2(d_1+d_2)^2}[(A_1d_1E_1 + A_2d_2E_2)N(x,t) + (A_1E_1 + A_2E_2)M(x,t)] + \frac{1}{(d_1+d_2)}[(\epsilon_1^{th}(x,t) + \epsilon_1^p(x,t)) - (\epsilon_2^{th}(x,t) + \epsilon_2^p(x,t))] \quad (17)$$

Boundary Conditions. Five boundary conditions are needed for solving the third-order differential Eq. (17) with respect to x, and two unknown (time-dependent) variables, the hoop force N_o and reaction moment M_o, at each instant of time.

$$\frac{dw(x,t)}{dx} = 0 \quad \text{at} \quad x = 0 \quad \text{and} \quad x = l;$$

$$\text{and} \quad w(x,t) = 0 \quad \text{at} \quad x = 0$$

$$u^o(x,t) = -l\epsilon_B \quad \text{at} \quad x = 0;$$

$$\text{and} \quad u^o(x,t) = 0 \quad \text{at} \quad x = l \quad (18)$$

where $x = 0$ and $x = l$, respectively, correspond to the junction with the rib and center section of the ligament; T_B and T_o are, respectively, the actual and (known) reference temperatures of the close-out wall; α_B is the linear coefficient of thermal expansion of the close-out wall material; and the close-out wall strain $\epsilon_B = \alpha_B T_B - \alpha_o T_o$ in Eq. (18) implies that the boundary constraint is affected by the displacement of the close-out wall.

Closed-Form Solution of the Sandwich Beam Model Equations. Applying Eq. (13) and the boundary conditions in Eqs. (18) into the governing Eqs. (17), the time-dependent reaction force N_o and moment M_o are obtained as:

$$N_o(t) = \tilde{C}\left(\tilde{I}_1^{th}(t) - \epsilon_B(t) + \frac{1}{l}\int_0^l \tilde{I}_1^p(x,t)dx\right)\Big/(\tilde{A}\tilde{C} - \tilde{B}^2) - \frac{\tilde{B}}{(d_1+d_2)}\left(\tilde{I}_2^{th}(t) + \frac{1}{l}\int_0^l (x,t)dx\right)\Big/(\tilde{A}\tilde{C} - \tilde{B}^2)$$

$$M_o(t) = -\frac{p(t)l^2}{3} + \tilde{B}\left(\tilde{I}_1^{th}(t) - \epsilon_B(t) + \frac{1}{l}\int_0^l \tilde{I}_1^p(x,t)dx\right) - \frac{\tilde{A}}{(d_1+d_2)}\left(\tilde{I}_2^{th}(t) + \frac{1}{l}\int_0^l \tilde{I}_2^p(x,t)dx\right) \quad (19)$$

where

$$\tilde{A} = \frac{A_1d_1^2E_1 + A_2d_2^2E_2}{A_1A_2E_1E_2(d_1+d_2)^2};$$

$$\tilde{B} = \frac{A_1d_1E_1 - A_2d_2E_2}{A_1A_2E_1E_2(d_1+d_2)^2}; \quad \text{and} \quad \tilde{C} = \frac{A_1E_1 + A_2E_2}{A_1A_2E_1E_2(d_1+d_2)^2}$$

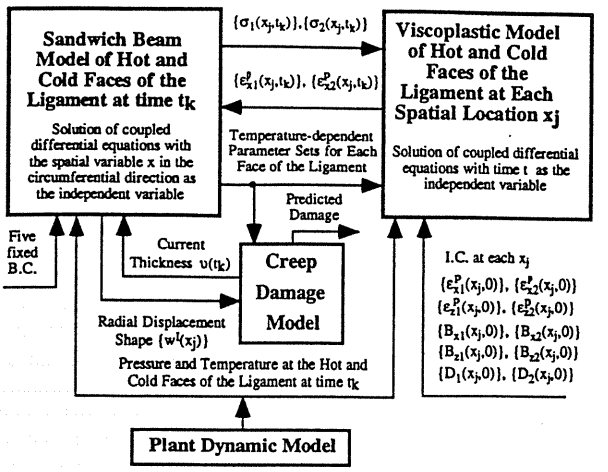

Fig. 4 Procedure for creep damage computation

$$\tilde{I}_1^{th} = \frac{(d_2\epsilon_1^{th} + d_1\epsilon_2^{th})}{(d_1+d_2)}; \quad \text{and} \quad \tilde{I}_1^p = \frac{(d_2\epsilon_1^p + d_1\epsilon_2^p)}{(d_1+d_2)}$$

$$\tilde{I}_2^{th} = (\epsilon_2^{th} - \epsilon_1^{th}); \quad \text{and} \quad \tilde{I}_2^p = (\epsilon_2^p - \epsilon_1^p) \quad (20)$$

Now the hoop stresses on the two thin faces of the sandwich beam, which are the inputs to the viscoplastic model, can be obtained in terms of the force and moment from Eqs. (12) as:

$$\sigma_1(x,t) = \frac{d_2N(x,t) - M(x,t)}{A_1(d_1+d_2)};$$

$$\text{and} \quad \sigma_2(x,t) = \frac{d_1N(x,t) + M(x,t)}{A_2(d_1+d_2)} \quad (21)$$

A closed-form solution of the radial deflection $w(x,t)$ at the mid-plane of the ligament can be obtained by substituting the boundary conditions in Eq. (18), and Eqs. (19) and (20) into the governing Eqs. (17) as:

$$w(x,t) = \frac{\tilde{C}x^2p(t)}{6}\left(l^2 - lx + \frac{x^2}{4}\right) + \frac{1}{(d_1+d_2)}\left(\frac{x^2}{2l}\int_0^l \tilde{I}_2^p d\xi - \int_0^x\int_0^\eta \tilde{I}_2^p d\xi d\eta\right) \quad (22)$$

The first term on the right-hand side of Eq. (22) represents the reversible components of the radial deflection that vanish in the absence of any pressure and temperature difference across the ligament when the cycle is completed. The second term on the right-hand side of Eq. (22) represents the deflection resulting from inelastic strain ratcheting induced by thermo-mechanical loading that contributes to permanent bulging-out of the ligament and progressive thinning of the coolant channel ligament. The second term of Eq. (22) generates the irreversible deflection at the mid-plane of the ligament that is denoted as $w^I(x,t)$, and is expressed as:

$$w^I(x,t) = \frac{1}{(d_1+d_2)}\left(\frac{x^2}{2l}\int_0^l \tilde{I}_2^p d\xi - \int_0^x\int_0^\eta \tilde{I}_2^p d\xi d\eta\right) \quad (23)$$

Differentiating Eq. (23) twice with respect to x, and changing the sign of the second derivative, the inelastic bending moment $M^I(x,t)$ which causes the permanent deflection due to creep ratcheting is obtained as:

$$M^I(x,t) = \frac{1}{(d_1+d_2)}\left[(\epsilon_2^p - \epsilon_1^p) - \frac{1}{l}\int_0^l (\epsilon_2^p - \epsilon_1^p)d\xi\right] \quad (24)$$

Integrals in Eqs. (23) and (24) are solved by conventional numerical methods such as Runge-Kutta. Fig. 4 presents a pro-

cedure for numerically solving the creep damage model in which the viscoplastic phenomena are represented in the state variable setting as a set of ordinary nonlinear differential equations with time as the independent variable. The relationships for inelastic deformation, tensile force and bending moment are obtained based on the five boundary conditions in Eq. (18) and the initial conditions of the plastic strains and deviatoric back stresses at each node. The number of nodes was chosen to be 11 for the half ligament in the simulation experiments.

Thinning Model of the Main Combustion Chamber Wall. Experimental studies by Hannum et al. (1976) show the evidence of incremental bulging-out and progressive thinning at the center of the ligament after each firing cycle for the OFHC copper material. Porowski et al. (1985) proposed a relationship for linear variations in the thickness of the coolant channel ligament, based on experimental observations of the deformed shapes. The total area of cross-section of the ligament is conserved under inelastic deformation because the ligament length does not change in the axial (y) direction and the principle of volume conservation holds under plastic deformation. Based on the details reported by Porowski et al. (1985), a simple geometric relationship for the incremental permanent deflection is derived as:

$$\frac{1}{2} l\delta_1(t) = \frac{1}{2}\left(l + \frac{a}{4}\right) w^I(l, t) = \frac{1}{2}\left(l + \frac{a}{2}\right)\delta_2(t) \quad (25)$$

where δ_1 and δ_2 are denoted as the respective deflections of the coolant side face and hot-gas side face at the center of the ligament; a is the rib width in the coolant channel. The time-dependent thinning, $\tau(t)$ of the ligament at its center is obtained as:

$$\tau(t) = \delta_1(t) - \delta_2(t) = \frac{\left(\frac{4l}{a} + 1\right) w^I(t)}{\frac{4l}{a}\left(\frac{2l}{a} + 1\right)} \quad (26)$$

The current ligament thickness is updated by subtracting the time-dependent thinning from the original thickness:

$$\vartheta(t) = \vartheta_0 - \tau(t) \quad (27)$$

and this information on $\vartheta(t)$ is fed back to Eq. (1) to calculate the sandwich model parameters as shown in Fig. 4.

Now we can define damage in terms of the normalized thinning with respect to the initial thickness, ϑ_o, of the ligament:

$$\bar{\tau}(t) = \tau(t)/\vartheta_o \quad (28)$$

Equation (28) and the supporting equations are used for synthesis of an optimal control policy in the second part (Dai and Ray, 1996).

Damage Analysis and Remaining Life Prediction of the Coolant Channel Ligament. The damage in the ligament is defined as a continuous function of time in the deterministic setting following the industrial practice of denoting damage in the scale of 0 to 1. The creep damage $D_{cr}(t)$ in the thrust chamber wall is thus expressed in terms of the current state of normalized thinning, $\bar{\tau}(t)$, of the ligament and its critical value, $\bar{\tau}^*$, beyond which the thinning process becomes unstable (i.e., the tensile rupture is imminent) as:

$$D_{cr}(t) = \frac{\bar{\tau}(t)}{\bar{\tau}^*} \quad (29)$$

The critical value $\bar{\tau}^*$ which is a positive fraction is experimentally determined for the ligament material (Kasper, 1984; Porowski et al., 1985) for a given range of thermo-mechanical

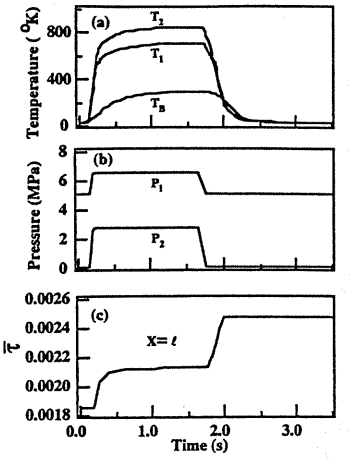

Fig. 5 Temperature/pressure profile for a cycle. (*a*) Temperature history; (*b*) pressure history; (*c*) normalized thinning $\bar{\tau}$ at $x = l$

load; $\bar{\tau}^*$ increases with increased ductility of the ligament material. It should be noted, however, that the definition of damage is not unique; the damage model may depend on the specific application.

The end of useful service period, t_f, at which the damage $D_{cr}(t_f)$ reaches unity (i.e., $\bar{\tau}(t_f) = \bar{\tau}^*$) denotes the total life of the thrust chamber wall ligament. Clearly, t_f is dependent on the complete history of thermo-mechanical load to which the ligament has been subjected. If the actual thermo-mechanical load is different from the anticipated load, the predicted total life t_f should be recalculated based on the load history up to the current time, t, and the updated profile of the anticipated load beyond time t. In that case, the predicted instant failure and hence the remaining service life $\Im$ becomes time-dependent.

$$\Im(t) = t_f(t) - t \quad (30)$$

Verification of the Sandwich Beam Model

The proposed sandwich beam model has been verified for both single-cycle and multi-cycle stress-strain behavior, where the temperature-dependent material parameters (e.g., coefficient of thermal expansion, modulus of elasticity, yield strength and ultimate strength) for oxygen free high conductivity (OFHC) copper have been taken from Hannum et al. (1976), and the material constants of the viscoplastic model from Freed and Verrilli (1988). The time history of the process variables including the wall temperatures at the hot-gas side, coolant side and closeout wall, and the pressure load acting on the ligament are shown in Figs. 5a and 5b for a single firing cycle having a duration of 3.5 seconds (Armstrong, 1981). Time history of the associated normalized thinning $\bar{\tau}$ is shown in Fig. 5c for a typical cycle where progressive thinning is observed for single cycle operation. The rapid increase in ligament thinning occurs during the heat-up and chill-down transients. At a thermo-mechanical loading transient or "primary" creep stage, the back stress lags behind the actual stress. This induces a large rate of change in the inelastic strains, which eventually causes a rapid increment of the ligament thinning. During temperature and pressure variations, the rate of change in the inelastic strains in the primary creep stage are more significant than those in the secondary creep stage under steady state when the impact of thermo-mechanical loading is essentially constant. Similar results for NARloy-Z, a copper-zirconium-silver alloy, have been reported in other publications (Dai and Ray, 1995; Ray and Dai, 1995).

Figure 6 shows profiles of the hoop stress and mechanical strain at the ligament center, averaged over the thickness, from the 2nd cycle to the 20th cycle. The stress profile in Fig. 6(a)

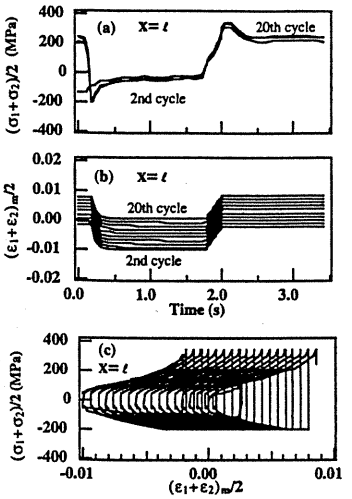

Fig. 6 Average cyclic hoop stress/strain profile at $x = l$, (*a*) Average cyclic hoop stress (MPa); (*b*) average cyclic mechanical hoop strain; (*c*) average cyclic stress/strain hysteresis loop.

remains practically unchanged after two or three transient cycles, and the mechanical strain increment per cycle in Fig. 6(*b*) becomes nearly constant. As the cycling continues, the inelastic strain becomes tensile even at the hot phase of the cycle due to strain ratcheting. Figure 6(*c*) shows that, after the first few cycles, the stress-strain hysteresis loops are repetitive with a constant average racheting rate of about 0.06 percent per cycle. The nonzero mean stress as seen in Fig. 6(*c*) results from unequal tensile and compressive loading and incomplete stress-strain loops due to temperature cycling. This thermo-mechanical creep ratcheting phenomenon, also discussed by Kasper (1984), is a consequence of cyclically varying mean stress and ligament temperature.

The failure mechanism of the coolant channel due to incremental bulging-out at each cycle for multiple cycles is illustrated by spatial distribution of the irreversible deflection, $w^I(x, t)$, defined in Eq. (23) and the bending moment, $M^I(t, x)$, defined in Eq. (24). Figure 7(*a*) shows the spatial profile of $w^I(x, t)$ after normalization with respect to the initial thickness, ϑ_o, of the ligament and Fig. 7(*b*) shows that of $M^I(t, x)$. As the cycles continue, the difference between the maximum and minimum values of $M^I(t, x)$ distribution increases and the shape of the spatial profile becomes more convex. This implies progressive bulging-out of the coolant channel ligament during both hot and cold phases as seen in Fig. 5(*c*).

Figure 8 compares the results of progressive thinning predicted by the sandwich beam model with those obtained from nonlinear finite element analysis as reported by Armstrong (1981). The thinning rate predicted by the sandwich model increases moderately during the initial cycles and then starts

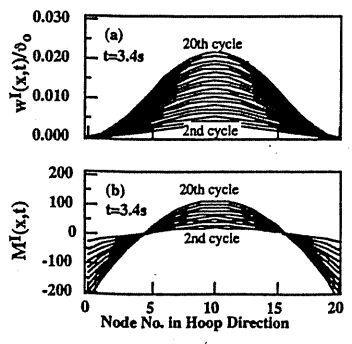

Fig. 7 Deflection and bending moment. (*a*) $w^I(x, t)/\vartheta_o$ at the cold phase of a cycle; (*b*) $M^I(t, x)$ at the cold Phase of a cycle.

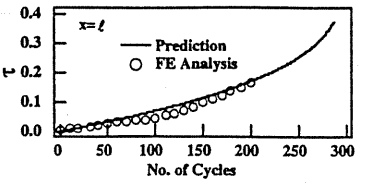

Fig. 8 Normalized thinning $\bar{\tau}$ Profile at $x = l$

accelerating. The rapid increase in thinning rate in Fig. 8 indicates that the ligament would fail by tensile rupture after about 250 cycles. This predicted life is qualitatively comparable with the experimental data on actual life of the main thrust chamber coolant channel wall, which ranges to 220 cycles (Quentmeyer, 1977). The analytical prediction is somewhat higher than the experimentally observed life possibly due to the fact that the life prediction model is based on uncertain parameters and several simplifying assumptions. These assumptions include absence of local stress concentrations, environmental/corrosion effect, pre-existing material defects, and the effects of low cycle fatigue.

Summary and Conclusions

This paper reports the development of a creep damage model in the coolant channel ligament of the main thrust chamber during both steady state and transient operations of a reusable rocket engine similar to the Space Shuttle Main Engine (SSME). This damage model is built upon the theories of sandwich beam and thermo-viscoplasticity. The modeling approach is based on analysis of the incremental bulging-out and progressive thinning of the ligament in each firing cycle by taking the effects of geometric deformation into consideration. This damage/life prediction model has been examined in terms of single-cycle and multi-cycle stress-strain behavior. The predicted results are in agreement with those obtained from the finite element analyses and experimental observation.

In contrast to the common practice of finite element analysis, the proposed model of creep damage in the coolant channel ligament offers a significant improvement in computational efficiency while the accuracy of analytical prediction is comparable. This model is not only suitable for on-line damage prediction as needed for damage-mitigating control but also capable of parametric studies for off-line synthesis of damage mitigating control systems. The advantages of this creep damage model are its simplicity, low computational cost, and capability to provide life prediction of the main thrust chamber for both intra-cycle and inter-cycle operations. However, the overall scope of this damage/life prediction model is limited compared to that of the finite-element model reported by Arya (1992).

An optimal control policy is formulated in the second part (Dai and Ray, 1996) for damage mitigating control of up-thrust transients of a reusable rocket engine. This control policy is synthesized via optimization of a cost functional of the plant dynamic performance without violating the damage constraints in the coolant channel ligament and the blades of the fuel and oxidizer turbines.

Acknowledgments

The authors acknowledge benefits of discussion with Professor Marc Carpino of Penn State University and Mr. Carl F. Lorenzo of NASA Lewis Research Center.

The research work reported in this paper has been supported in part by:
NASA Lewis Research Center under Grant No. NAG 3-1240.
NASA Lewis Research Center under Grant No. NAG 3-1673.
National Science Foundation under Research Grant No. ECS-9216386. National Science Foundation under Research Grant No. DMI-9424587. Office of Naval Research under Grant No.

N00014-90-J-1513. Electric Power Research Institute under Contract No. EPRI RP8030-5. National Science Foundation under Research Equipment Grant No. MSS-9112609.

References

Allen, D. H. and Beek, J. M., 1984, "On the Use of Internal State Variables in Thermoviscoplastic Constitutive Equations," *Symposium on Nonlinear Constitutive Relations for High Temperature Application,* NASA Lewis Research Center, June 15–17, pp. 83–101.

Armstrong, W. H., 1979, *Structural Analysis of Cylindrical Thrust Chamber,* Final Report, Volume I, NASA CR-159552, Contract NASA-21361, NASA Lewis Research Center, March.

Armstrong, W. H., 1981, *Structural Analysis of Cylindrical Thrust Chamber,* Final Report, Volume II, NASA CR-165241, Contract NASA-21953, NASA Lewis Research Center, March.

Arnold, S. M., Robinson, D. N., and Saleeb, A. F., 1989, "Creep Buckling of Cylindrical Shell Under Variable Loading," *Journal of Engineering Mechanics,* Vol. 115, No. 5, May–Aug., pp. 1054–1075.

Arya, V. K., 1992, "Nonlinear Structural Analysis of Cylindrical Thrust Chambers Using Viscoplastic Models," *Journal of Propulsion and Power,* Vol. 8, No. 3, May–June, pp. 598–604.

Chen, K. S., Lindholm, U. S., Bodner, S. R., and Walker, K. P., 1984, "A Survey of Unified Constitutive Theories," *Symposium on Nonlinear Constitutive Relations for High Temperature Application,* NASA Lewis Research Center, June 15–17, pp. 1–23.

Dai, X. and Ray, A., 1995, "Life Prediction of the Thrust Chamber Wall of a Reusable Rocket Engine," *AIAA Journal of Propulsion and Power,* Vol. 11, No. 6, pp. 1279–1287.

Dai, X. and Ray, A., 1996, "Damage Mitigating Control of a Reusable Rocket Engine: Part II: Synthesis of an Optimal Policy," published in this issue, pp. 000.

Freed, A. D., 1988, *Structure of a Viscoplastic Theory,* NASA TM-100749, Lewis Research Center, Prepared for the Summer Annual Meeting Symposium "Constitutive Equations and Life Prediction Models for High Temperature Applications," Sponsored by ASME, Berkeley, CA, June 20–22.

Freed, A. D., and Verrilli, M. J., 1988, "A Viscoplastic Theory Applied to Copper," NASA TM-100831 NASA Lewis Research Center, Aug.–Sept.

Hannum, N. P., Kasper, H. J., and Pavli, A. J., 1976, *Experimental and Theoretical Investigation of Fatigue Life in Reusable Rocket Thrust Chambers,* NASA TM X-73413, Lewis Research Center, July.

Kasper, H. J., 1984, "Thrust Chamber Life Prediction," NASA Conference Publication 2372, *Advanced high pressure O2/H2 technology,* Proceedings of a conference at George C. Marshall Flight Center, Huntsville, Alabama, June 27–29, pp. 36–43.

Lorenzo, C. F., and Merrill, W. C., 1991a, "Life Extending Control: A Concept Paper," *American Control Conference,* Boston, MA, June, pp. 1080–1095.

Lorenzo, C. F., and Merrill, W. C., 1991b, "An Intelligent Control System for Rocket Engines: Need, Vision, and Issues," *Control Systems Magazine,* Vol. 12, No. 1. Jan., pp. 42–46.

McDowell, D. L., 1992, "A Nonlinear Kinematic Hardening Kinematic Theory for Cyclic Thermoplasticity and Thermoviscoplasticity," *International Journal of Plasticity,* Vol. 8, pp. 695–728.

Noll, T., Austin, E., Donley, S., Graham, G., Harris, T., Kaynes, I., Lee, B., and Sparrow, J., 1991, "Impact of Active Controls Technology on Structural Integrity," 32nd AIAA/ASME/ASCE/AHS/ASC *Structures, Structural Dynamics, and Materials Conference,* Baltimore, MD, April, pp. 1869–1878.

Porowski, J. S., O'Donnell, W. J., Badlani, M. L., and Kasraie, B., 1985, "Simplified Design and Life Prediction of Rocket Thrust Chambers," *Journal of Spacecraft,* March–April, Vol. 22, pp. 181–187.

Pugh, C. E. and Robinson, D. N., 1978, "Some Trends in Constitutive Equation Model Development for High-Temperature Behavior of Fast-Reactor Structural Alloys," *Journal of Nuclear Engineering and Design,* Vol. 48, pp. 269–276.

Quentmeyer, R. J., 1977, "Experimental Fatigue Life Investigation of Cylindrical Thrust Chambers," NASA TM X-73665, Lewis Research Center, July.

Ray, A. and Wu, M-K., 1994a, "Fatigue Damage Control of Mechanical Systems," *SMART Materials and Structures,* Vol. 3, No. 1, March, pp. 47–58.

Ray, A. and Wu, M-K., 1994b, "Damage-Mitigating Control of Space Propulsion Systems for High Performance and Extended Life," NASA CR-194470, Lewis Research Center, March.

Ray, A., Wu, M-K., Carpino, M., and Lorenzo, C. F., 1994a, "Damage-Mitigating Control of Mechanical Systems: Part I—Conceptual Development and Model Formulation," ASME JOURNAL OF DYNAMIC SYSTEMS, MEASUREMENT, AND CONTROL, Vol. 116, No. 3, September, pp. 437–447.

Ray, A., Wu, M-K., Carpino, M., and Lorenzo, C. F., 1994b, "Damage-Mitigating Control of Mechanical Systems: Part II—Formulation of an Optimal Policy and Simulation," ASME JOURNAL OF DYNAMIC SYSTEMS, MEASUREMENT, AND CONTROL, Vol. 116, No. 3, September, pp. 448–455.

Ray, A., Dai, X., Wu, M-K., Carpino, M. and Lorenzo, C. F., 1994c, "Damage-Mitigating Control of a Reusable Rocket Engine," *AIAA Journal of Propulsion and Power,* Vol. 10, No. 2, Mar./Apr., pp. 225–234.

Ray, A., and Dai, X., 1995, "Damage-Mitigating Control of a Reusable Rocket Engine for High Performance and Extended Life," NASA Contractor Report 4640, NASA Lewis Research Center.

Robinson, D. N., and Arnold, S. M., 1990, "Effects of State Recovery on Creep Buckling Under Variable Loading," ASME *Journal of Applied Mechanics,* Vol. 57, June, pp. 313–320.

Stubstad, J. M. and Simitses, G. J., 1987, "Creep Analysis of Beams and Arches Based on A Hereditary Visco-Elastic-Plastic Constitutive Law," *Constitutive Modeling for Engineering Materials With Applications,* Vol. 153, pp. 1–15.

Sutton, G. P., 1992, *Rocket Propulsion Elements, an Introduction to the Engineering of Rockets,* Wiley Interscience, New York.